Plavnoite, a new K–Mn member of the zippeite group from Jáchymov, Czech Republic

Jakub Plášil[1,*], Pavel Škácha[2], Jiří Sejkora[3], Anthony R. Kampf[4], Radek Škoda[5], Jiří Čejka[3], Jan Hloušek[6,†], Anatoly V. Kasatkin[7], Radim Pavlíček[8] and Karel Babka[9]

[1] Institute of Physics ASCR, v.v.i., Na Slovance 1999/2, 18221 Praha 8, Czech Republic
*Corresponding author, e-mail: plasil@fzu.cz
[2] Mining Museum Příbram, 261 01 Příbram VI Březové Hory, Czech Republic
[3] Department of Mineralogy and Petrology, National Museum, Cirkusová 1740, 193 00 Praha 9, Czech Republic
[4] Mineral Sciences Department, Natural History Museum of Los Angeles County, 900 Exposition Boulevard, Los Angeles, CA 90007, USA
[5] Department of Geological Sciences, Faculty of Science, Masaryk University, Kotlářská 2, 611 37 Brno, Czech Republic
[6] Jáchymov, Czech Republic
[7] Fersman Mineralogical Museum of the Russian Academy of Sciences, Leninsky Prospekt 8-2,117071 Moscow, Russia
[8] Havlíčkova388, Unhošt 27351, Czech Republic
[9] Na Vysluní 1154, CZ-277 11 Neratovice, Czech Republic
[†] Deceased 27 April 2014

Abstract: The new mineral plavnoite (IMA2015-059), ideally $K_{0.8}Mn_{0.6}[(UO_2)_2O_2(SO_4)]\cdot3.5H_2O$, is a member of the zippeite group. It was found in the Plavno mine, in the eastern part of the Jáchymov ore district, Western Bohemia, Czech Republic, where it occurs as a supergene alteration phase formed by hydration–oxidation weathering of uraninite in hydrothermal U-veins. It was found to be associated with marécottite, magnesiozippeite, blatonite and gypsum. The mineral occurs as reddish to reddish-orange thin blades, elongated on [0 0 1] and flattened on {0 1 0}, which are intergrown in globular aggregates up to 0.5 mm across. Crystals are transparent with a vitreous to silky lustre. The streak is pale orange. The mineral is non-fluorescent under both long- and short-wave ultraviolet (UV) radiation. The Mohs hardness is about 2. Crystals are brittle with perfect {0 1 0} cleavage and uneven fracture. The density calculated from the empirical formula is $4.926\,\mathrm{g\,cm^{-3}}$. Optically, plavnoite is biaxial $(+)$, with $\alpha = 1.740(5)$, $\beta = 1.770(5)$, $\gamma = 1.850(5)$ (measured in white light). The measured $2V$ is $64.6(4)°$; the calculated $2V$ is $65.3°$. Dispersion could not be observed; no pleochroism was observed. Electron-microprobe analyses yielded the empirical formula (based on 2 U atoms per formula unit, apfu) $K_{0.77}(Mn_{0.51}Zn_{0.04}Ni_{0.03}Mg_{0.02})_{\Sigma0.60}[(UO_2)_2O_{1.08}(OH)_{0.92}(SO_4)_{0.96}(SiO_4)_{0.24}](H_2O)_{3.50}$. Plavnoite is monoclinic, $C2/c$, $a = 8.6254(16)$, $b = 14.258(3)$, $c = 17.703(4)$ Å, $\beta = 104.052(18)°$, $V = 2122.0(8)$ Å^3 and $Z = 8$. The structure ($R_1 = 4.99\%$ for 989 reflections with $I > 3\sigma[I]$) contains UO_7 pentagonal bipyramids and SO_4 tetrahedra forming sheets of the well-known zippeite topology. The interlayer region contains infinite zig–zag chains of corner-sharing $Mn^{2+}\Phi_6$ octahedra ($\Phi = O$, H_2O) with K-centred polyhedra. The K atom sits at the partially occupied, mixed K/O site, the non-shared corner of the Mn2 octahedron. The mineral is named after the type locality − the Plavno mine.

Key-words: plavnoite; uranyl sulfate hydrate; new mineral; zippeite group; crystal structure; chemical composition.

1. Introduction

Plavnoite, a K–Mn member of the zippeite group, is a new uranyl sulfate mineral found at Jáchymov, Czech Republic. Members of this group, referred to as *zippeites* in the following, are common alteration products after uraninite and sulfides in oxide zones of many uranium deposits (Krivovichev & Plášil, 2013; Plášil, 2014). Members of the zippeite group are paragenetically, chemically (Frondel *et al.*, 1976; Krivovichev & Plášil, 2013; Plášil, 2014) and structurally related (Burns *et al.*, 2003; Burns, 2005; Krivovichev & Plášil, 2013). Detailed information on the crystallography and crystal chemistry of this mineral group has been given elsewhere (*e.g.* Burns *et al.*, 2003; Brugger *et al.*, 2003, 2006; Peeters *et al.*, 2008; Plášil *et al.*, 2011a and b; Plášil & Škoda, 2015). Structurally, these minerals differ in having distinct symmetries (triclinic to orthorhombic) and space groups; however, they all possess structures based on sheets of the same topology, the zippeite topology (Burns, 2005), giving a U:S ratio equal to 2:1. Chemically, *zippeites*

are hydrated oxo–hydroxo sulfates of uranyl containing in their structures monovalent (K^+, Na^+ and NH_4^+), divalent (Mg^{2+}, Ca^{2+}, Zn^{2+}, Co^{2+}, Ni^{2+} and Cu^{2+}) and trivalent (Y^{3+} and REE^{3+}) cations (Frondel *et al.*, 1976; Brugger *et al.*, 2003; Burns *et al.*, 2003; Plášil *et al.*, 2011a and b, 2012). There is no general valid formula for the whole group. The formula of zippeite proper can be expressed as $K_x[(UO_2)_4(SO_4)_2O_x(OH)_{4-x}](H_2O)_{6-x}$, where $x \approx 2$ in the natural material and $x \approx 3$ in synthetic material (Burns *et al.*, 2003; Plášil *et al.*, 2011a). The general formula of the M^{2+}-dominant members of the zippeite group, except the mineral pseudojohannite (which contains Cu^{2+}) and marécottite (containing Mg^{2+}), can be expressed as $M_x^{2+}[(UO_2)_{2x}O_{2x}(SO_4)_x](H_2O)_{3.5}$ (Burns *et al.*, 2003; Plášil *et al.*, 2012). The structure of natural magnesiozippeite (Plášil *et al.*, 2012), the monoclinic Mg member, differs from the structure of the synthetic phase (Burns *et al.*, 2003). There are additional Mg-containing synthetic phases distinct from magnesiozippeite by their symmetry and composition (Burns *et al.*, 2003). The mineral marécottite (Brugger *et al.*, 2003; Plášil & Škoda, 2015) is a triclinic Mg-bearing member with the ideal formula $Mg_3[(UO_2)_4O_3(OH)(SO_4)_2]_2(H_2O)_{28}$. The mineral pseudojohannite is unique both structurally and chemically due to the presence of Cu^{2+}, which undergoes Jahn–Teller distortions (Plášil *et al.*, 2012). Pseudojohannite is triclinic (space group P-1), and its chemical formula is $Cu_3(OH)_2[(UO_2)_4O_4(SO_4)_2](H_2O)_{12}$ (Plášil *et al.*, 2012). There is only one member of the group that contains trivalent cations, the mineral sejkoraite-(Y), which is triclinic (space group P-1) with the ideal formula $Y_3[(UO_2)_8O_7OH(SO_4)_4](OH)_2(H_2O)_{24}$ (Plášil *et al.*, 2011b). Plavnoite is a new member of this group, chemically and structurally similar to the monoclinic M^{2+}-bearing members. Formally, the classification and nomenclature of the group that have been established by Frondel *et al.* (1976) are still used; however, novel studies make clear that an updated, new classification of this group is needed.

Plavnoite is named after the type locality, the Plavno mine. The new mineral and its name were approved by the Commission on New Minerals, Nomenclature and Classification of the International Mineralogical Association (IMA2015-059). There are three cotype specimens. One is deposited in the collections of the National Museum in Prague, Department of Mineralogy and Petrology, Cirkusová 1740, Praha 9, Czech Republic under the catalogue number P1P 4/2015. The second one is deposited in the collections of the Natural History Museum of Los Angeles County, 900 Exposition Boulevard, Los Angeles, CA 90007, USA, catalogue number 65588. The third cotype is deposited in the Fersman Mineralogical Museum of the Russian Academy of Sciences, registration number 4740/1.

2. Occurrence

Plavnoite was found on several samples originating from the Plavno mine, which is located in the south-eastern part of the Jáchymov ore district, Czech Republic. A description of the Jáchymov ore district and its geological

Fig. 1. A typical crystal aggregate of plavnoite overgrowing a clayey-quartz gangue. Field of view is 2.5-mm wide, photograph by P. Škácha. (Online version in colour)

setting have been given in detail elsewhere (*e.g.* Ondruš *et al.*, 1997, 2003; Hloušek *et al.*, 2014). The Jáchymov ore district is a classic example of the Variscan hydrothermal vein type of deposit, the so-called five-element formation, Ag–Bi–Co–Ni–U. Jáchymov is the type locality for 46 minerals, and more than 430 minerals have been identified from there.

The samples were found underground on the vein no. 13 at the 2nd level of the Vladimír shaft of the Plavno mine. Along with plavnoite, superior crystals of marécottite, used for the X-ray studies by Plášil & Škoda (2015), as well as magnesiozippeite and blatonite were found. Samples consist of highly haematitized, clayey material (resembling mylonitic material) of dark reddish-brown colour. Hundreds of isolated crystal aggregates of marécottite, magnesiozippeite and plavnoite were found in cracks within the clayey material and surrounding rocks. The clayey material is a mixture of a mica-related phase, quartz, haematite and gypsum. Detailed information on geological settings and the type of mineralization found at the locality is given in the above-mentioned papers.

3. Physical and optical properties

Plavnoite forms reddish-orange to orange thin blades, up to about 50-μm long, tightly packed into globular aggregates, up to about 0.5 mm across (Figs. 1 and 2). Crystals are elongated on $[0\,0\,1]$ and flattened on $\{0\,1\,0\}$. The prism forms include $\{1\,0\,0\}$, $\{0\,1\,0\}$, $\{0\,1\,1\}$ and $\{0\,\overline{1}\,1\}$ (Fig. 3). Twinning is common on $\{1\,0\,0\}$. Crystals are transparent with a vitreous to silky lustre. The streak is pale orange. The mineral is non-fluorescent under both long- and short-wave UV radiation. The Mohs hardness is about 2. Crystals are brittle with perfect $\{0\,1\,0\}$ cleavage and uneven fracture. The density could not be measured because of the paucity of pure material for physical measurement. The calculated density is 4.926 g cm^{-3} based on the empirical formula.
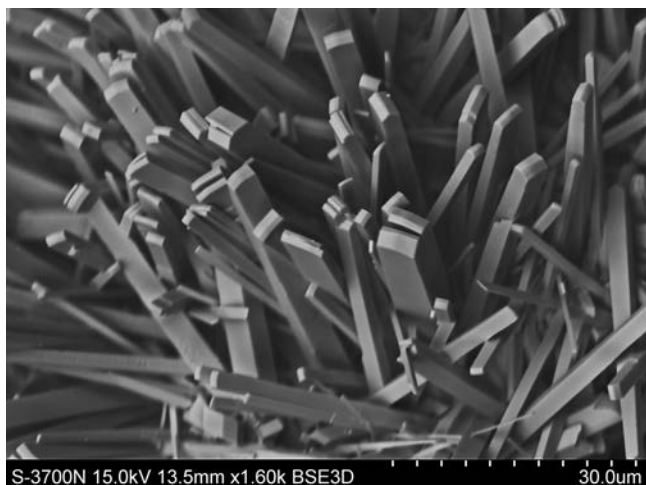
Fig. 2. Blades of plavnoite (backscattered-electron image, Hitachi S-3700N).
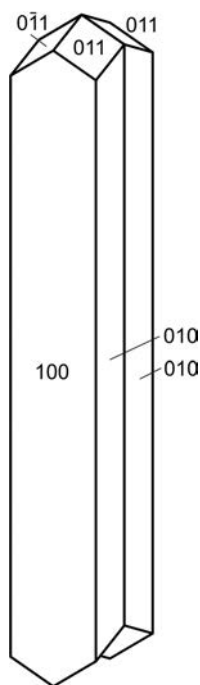

Fig. 3. Idealized crystal drawing of twinned plavnoite; clinographic projection in non-standard orientation.

Optically, plavnoite is biaxial (+), with $\alpha = 1.740(5)$, $\beta = 1.770(5)$, $\gamma = 1.850(5)$ (measured in white light). The measured $2V$ based on extinction data collected on a spindle stage and analysed using EXCALIBRW is 64.6 (4)°; the calculated $2V$ is 65.3°. Dispersion could not be observed. No pleochroism was observed.

4. Chemical composition

A crystal aggregate of plavnoite was analysed using a Cameca SX100 electron microprobe (Masaryk University, Brno), operating in wavelength-dispersive mode with an accelerating voltage of 15 kV, beam current of 2 nA and a 15-μm beam diameter. We use a wide beam and a low

current to prevent from volatilization of elements such as K (*cf.* Plášil *et al.*, 2014a). The following X-ray lines and standards were used: $K\alpha$ lines: Mg (Mg_2SiO_4), S ($BaSO_4$), K and Si (sanidine), Mn (spessartite), Zn (ZnO) and Ni (Ni_2SiO_4); $M\alpha$ line: U (uranophane). Other elements, such as Al, Ca, Co, Cu, Fe, Na, Pb, Ba, Y, As, P, V and F, were also sought but were below the detection limits (~0.05–0.15 wt.% under the analytical conditions used). The peak counting times were 10–20 s, and the counting time for each background point was 50 % of the time for peak. The measured intensities were converted to elemental concentrations using the PAP programme (Pouchou & Pichoir, 1985). The low total sums of the corresponding analyses are caused by the instrumental difficulties (crystal size much smaller than the beam size; necessity to use a defocused beam to prevent K volatilization) and the imperfection of the polishing. Table 1 gives the chemical composition obtained for the plavnoite-type sample (five-point analyses), with H_2O contents calculated assuming charge balance (OH) and ideally $3.5H_2O$ per formula unit (pfu). The empirical formula calculated on the basis of 2 U atoms pfu is $K_{0.77}(Mn_{0.51}Zn_{0.04}Ni_{0.03} \quad Mg_{0.02})_{\Sigma0.60} \quad [(UO_2)_2O_{1.08} (OH)_{0.92}(SO_4)_{0.96}(SiO_4)_{0.24}](H_2O)_{3.50}$. The elevated Si contents may be a contribution by the sample matrix due to the very small size of the crystals from the holotype specimen available for analysis. Indeed, as better material became available (see below, Table 2), it showed no Si in the analyses. The ideal formula is $K_{0.8}Mn_{0.6}[(UO_2)_2 O_2(SO_4)]\cdot3.5H_2O$, which requires K_2O 4.74, MnO 5.35, SO_3 10.06, UO_3 71.91 and H_2O 7.93, total 99.99 wt.% (rounding errors).

Five additional samples of plavnoite were analysed (Table 2) in order to check for chemical variability. Their chemical composition is in general close to that of the type sample. The empirical analytical totals show a large range (77.03–96.65 wt.%), which appears to be related to the size of analysed groups of plavnoite crystals. According to the available data, plavnoite chemistry ranges from $K_{0.53} Mn_{0.57}$ to $K_{0.8}Mn_{0.58}$ (Fig. 4).

The Gladstone–Dale compatibility index $1 - (K_P/K_C)$ is 0.011 (superior) for the empirical formula of the type sample and the density calculated from the powder X-ray diffraction data.

4.1. Raman spectroscopy

The Raman spectrum was recorded with a Thermo-Scientific DXR Raman microscope interfaced to an Olympus microscope (objective 50×) in the spectral region 50–4000 cm^{-1} with a nominal resolution of ~5 cm^{-1}. The power of the frequency-stabilized single-mode diode laser (532 nm) impinging on the sample was about 2 mW. The spectrometer was calibrated with a software-controlled calibration procedure (Omnic 8 software) using multiple neon emission lines (wavelength calibration), multiple polystyrene Raman bands (laser frequency calibration) and standardized white-light sources (intensity calibration). Spectral manipulation,

Table 1. Results of WDS analyses of plavnoite-type sample from Jáchymov.

Constituent	wt.%	Range	Stand. dev.	Norm. wt.%	Probe standard
K_2O	3.77	3.64–4.00	0.14	4.47	Sanidine
MnO	3.75	3.43–4.21	0.31	4.45	Spessartine
NiO	0.21	0.00–0.40	0.19	0.24	Ni_2SiO_4
ZnO	0.35	0.09–0.52	0.21	0.42	ZnO
MgO	0.08	0.01–0.18	0.08	0.10	Mg_2SiO_4
SiO_2	1.52	0.23–2.81	0.91	1.81	Sanidine
SO_3	7.93	7.27–8.61	0.64	9.41	Barite
UO_3	59.29	56.59–61.74	2.25	70.34	Uranophane
H_2O*	7.40	–	–	8.77	–
Total	84.30			100.00	

* H_2O content was calculated on the basis of charge balance and $3.5H_2O$ pfu.

Table 2. Chemical composition of additional plavnoite samples from Jáchymov.

Sample	Ideal	Type	A	B	C	D	E
n		5	5	4	6	8	7
K_2O	4.74	3.77	2.68	2.96	3.63	4.32	3.33
MgO	0.00	0.08	0.00	0.04	0.03	0.08	0.02
CuO	0.00	0.00	0.13	0.00	0.32	0.00	0.00
CoO	0.00	0.00	0.05	0.00	0.21	0.10	0.03
NiO	0.00	0.21	0.10	0.00	0.03	0.03	0.00
MnO	5.35	3.75	3.62	4.26	4.20	4.11	3.61
ZnO	0.00	0.35	0.38	0.42	0.03	0.30	0.04
Al_2O_3	0.00	0.00	0.00	0.00	0.00	0.01	0.11
SiO_2	0.00	1.52	0.00	0.00	0.02	0.00	0.10
SO_3	10.06	7.93	7.16	8.71	9.17	9.68	8.24
UO_3	71.91	59.29	56.64	64.67	66.77	70.12	59.52
H_2O*	7.92	7.40	6.27	7.33	7.53	7.90	6.84
Total	99.99	84.30	77.03	88.40	91.95	96.65	81.85
K	0.801	0.773	0.575	0.557	0.660	0.748	0.680
Mg	0.000	0.020	0.000	0.008	0.006	0.016	0.006
Cu	0.000	0.000	0.016	0.000	0.035	0.000	0.000
Co	0.000	0.000	0.007	0.000	0.024	0.010	0.004
Ni	0.000	0.026	0.013	0.000	0.004	0.004	0.000
Mn	0.600	0.510	0.516	0.532	0.507	0.472	0.490
Zn	0.000	0.041	0.047	0.046	0.003	0.030	0.005
Al	0.000	0.000	0.000	0.000	0.000	0.002	0.020
SiO_4	0.000	0.244	0.000	0.000	0.003	0.000	0.016
SO_4	1.000	0.956	0.903	0.962	0.982	0.986	0.989
UO_2	2.000	2.000	2.000	2.000	2.000	2.000	2.000
H	6.999	7.922	7.031	7.197	7.157	7.153	7.293
OH*	0.000	0.922	0.031	0.197	0.157	0.153	0.293
H_2O*	3.5	3.5	3.5	3.5	3.5	3.5	3.5

* H_2O contents were calculated on the basis of charge balance (OH) and ideal $3.5H_2O$; n − number of spot analyses; coefficients of empirical formula were calculated on the basis of 2 U pfu.

such as background correction, was done with Omnic 8 software. The tentative assignment of the plavnoite spectrum was done based on papers by Čejka (1999) and Plášil et al. (2010).

The Raman spectrum of plavnoite is shown in Fig. 5. Raman bands at 3533 and 3385 cm^{-1} are assigned to νO–H stretching vibrations of symmetrically non-equiva-lent hydrogen-bonded H_2O molecules. The O_{donor}–$O_{acceptor}$ distances of the corresponding hydrogen bonds, inferred from the empirical relation given by Libowitzky (1999), are ~3.0 and ~2.8 Å. A weak band at 1630 cm^{-1} is attributed to the δ H–O–H bending vibration. Bands at 1106 and 1027 cm^{-1} are attributed to the ν_3 SO_4^{2-} triply degenerate antisymmetric stretching and ν_1 SO_4^{2-}
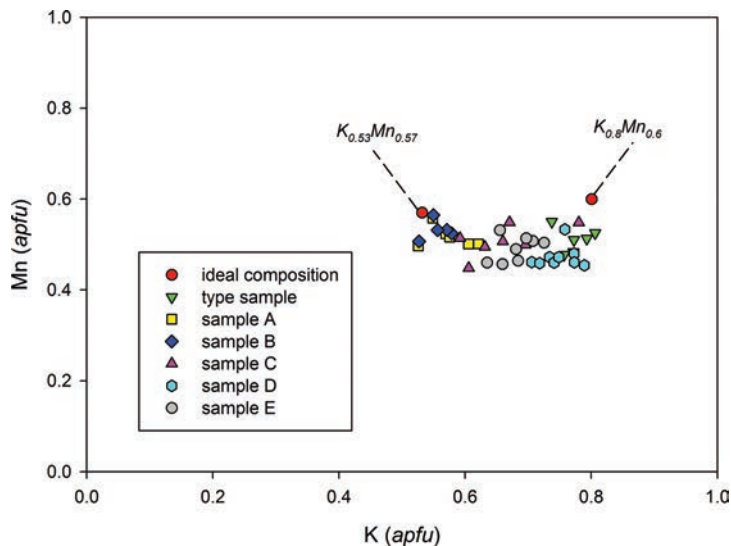
Fig. 4. Metal cation contents (expressed as apfu) of the analysed plavnoite samples (data from Table 2). (Online version in colour)
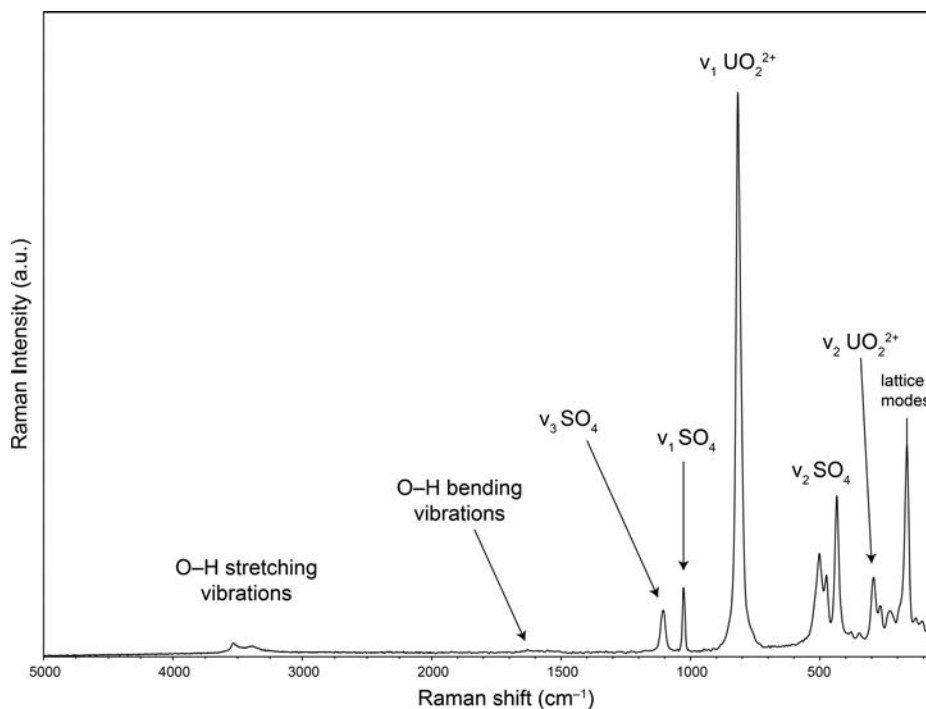

Fig. 5. Raman spectrum of plavnoite.

symmetric stretching vibrations, respectively. The ν_1 UO_2^{2+} symmetric stretching vibration is assigned to the very strong band at $817\,cm^{-1}$. The inferred U–O bond length obtained from the empirical relation given by Bartlett & Cooney (1989) is $\sim 1.79\,\text{Å}$. Bands at 502, 475 and $435\,cm^{-1}$ were assigned to the split doubly degenerate $\nu_2\ SO_4^{2-}$ bending vibrations. Raman bands at 377 and $348\,cm^{-1}$ are attributed to the stretching U–O_{ligand} vibrations, and the bands at 292 and $267\,cm^{-1}$ to the split doubly degenerate $\nu_2\ (\delta)\ UO_2^{2+}$ bending vibrations. The bands at 229, 164, 129 and $106\,cm^{-1}$ are assigned to lattice modes.

4.2. Powder X-ray diffraction

Powder X-ray diffraction data for plavnoite (Table 3) were obtained at room temperature using a PANalytical Empyrean powder diffractometer equipped with a Cu X-ray tube and PIXcel3D solid-state detector. The powder data were measured using Debye–Scherrer geometry, with $CuK\alpha_{1,2}$ provided by the focusing Göbel-mirror optics. The sample was mounted in a boron-glass capillary (0.3 mm in diameter) and scanned over the 2θ range from $4°$ to $80°$ with a step size of $0.013°\ 2\theta$ and a counting time of $10\,s$ per step (accumulation of 20 patterns during a total

Table 3. Powder diffraction data for plavnoite from Jáchymov (strongest lines in bold; *d* values quoted in Å).

I_{obs}	d_{obs}	d_{calc}	h	k	l
27	**8.590**	**8.595**	**0**	**0**	**2**
100	**7.133**	**7.138**	**0**	**2**	**0**
3	6.203	6.205	$\bar{1}$	1	2
13	5.489	5.491	0	2	2
8	4.296	4.297	0	0	4
9	4.185	4.185	2	0	0
		4.184	$\bar{2}$	0	2
2	4.135	4.137	1	3	0
1	4.089	4.088	$\bar{1}$	1	4
5	3.914	3.915	$\bar{1}$	3	2
5	3.680	3.682	0	2	4
9	3.610	3.610	2	2	0
25	**3.565**	**3.569**	**0**	**4**	**0**
36	**3.446**	**3.448**	**2**	**0**	**2**
		3.445	**$\bar{2}$**	**0**	**4**
3	3.295	3.296	0	4	2
47	**3.104**	**3.105**	**2**	**2**	**2**
		3.103	**$\bar{2}$**	**2**	**4**
14	2.8650	2.8649	0	0	6
2	2.8155	2.8163	1	3	4
1	2.8079	2.8099	$\bar{3}$	1	2
1	2.7444	2.7455	0	4	4
2	2.7158	2.7156	$\bar{2}$	4	0
1	2.7124	2.7151	$\bar{2}$	4	2
1	2.6991	2.7022	1	5	0
2	2.6879	2.6875	$\bar{2}$	0	6
15	**2.6582**	**2.6587**	**0**	**2**	**6**
13	2.6372	2.6376	$\bar{1}$	5	2
1	2.5218	2.5219	1	5	2
2	2.5172	2.5170	2	2	4
1	2.4898	2.4903	1	1	6
10	2.4799	2.4797	2	4	2
		2.4786	$\bar{2}$	4	4
1	2.4554	2.4551	$\bar{3}$	3	2
<1	2.4463	2.4461	3	1	2
<1	2.4067	2.4069	3	3	0
2	2.3784	2.3792	0	6	0
2	2.2927	2.2930	0	6	2
<1	2.2675	2.2676	$\bar{3}$	1	6
6	2.2343	2.2341	0	4	6
1	2.2106	2.2108	1	5	4
1	2.2014	2.2012	3	3	2
<1	2.1883	2.1885	$\bar{1}$	1	8
6	2.1575	2.1571	$\bar{4}$	0	2
2	2.1499	2.1487	0	0	8
		2.1469	$\bar{2}$	4	6
3	2.1348	2.1349	2	0	6
2	2.1327	2.1334	$\bar{2}$	0	8
2	2.0927	2.0918	$\bar{4}$	0	4
<1	2.0806	2.0815	0	6	4
6	2.0666	2.0684	$\bar{3}$	3	6
		2.0649	$\bar{4}$	2	2
3	2.0577	2.0575	0	2	8
3	2.0459	2.0474	$\bar{1}$	5	6
		2.0454	2	2	6
		2.0440	$\bar{2}$	2	8
4	2.0090	2.0081	4	2	0
		2.0074	$\bar{4}$	2	4
1	1.9813	1.9813	1	7	0
2	1.7826	1.7821	2	6	4
1	1.7792	1.7792	3	1	6
2	1.7614	1.7613	1	7	4
1	1.7571	1.7571	$\bar{1}$	1	10
1	1.7506	1.7499	$\bar{1}$	5	8
4	1.7471	1.7470	2	0	8
		1.7459	$\bar{2}$	0	10
4	1.7239	1.7240	4	0	4
3	1.7191	1.7190	0	0	10
<1	1.7008	1.7007	3	5	4
8	1.6965	1.7470	2	2	8
		1.7459	$\bar{2}$	2	10
4	1.6920	1.6942	$\bar{5}$	1	4
5	1.6758	1.6780	3	3	6
		1.6758	4	2	4
		1.6745	$\bar{4}$	2	8
4	1.6710	1.6712	0	2	10
<1	1.6618	1.6616	$\bar{3}$	7	2
1	1.6469	1.6464	3	7	0
1	1.6419	1.6413	$\bar{2}$	8	2
<1	1.6210	1.6211	1	5	8
1	1.6173	1.6167	$\bar{3}$	7	4
<1	1.6063	1.6061	$\bar{5}$	3	4
1	1.5986	1.5981	$\bar{4}$	6	2
		1.5946	0	6	8
1	1.5886	1.5883	$\bar{2}$	6	8
1	1.5850	1.5847	2	8	2
		1.5845	$\bar{2}$	8	4
1	1.5708	1.5710	$\bar{4}$	6	4
3	1.5691	1.5691	2	4	8
		1.5683	$\bar{2}$	4	10
<1	1.5585	1.5584	1	9	0
3	1.5525	1.5523	$\bar{4}$	4	4
		1.5513	$\bar{4}$	4	8
2	1.5481	1.5487	0	4	10
2	1.5462	1.5457	$\bar{1}$	9	2
1	1.5245	1.5249	$\bar{3}$	7	6
1	1.5208	1.5214	1	9	2
1	1.5148	1.5146	0	8	6
1	1.5002	1.5002	$\bar{1}$	7	8
1	1.4972	1.4982	4	6	2
<1	1.4938	1.4937	5	3	2
1	1.4881	1.4882	$\bar{4}$	2	10
1	1.4691	1.4688	3	7	4
1	1.4651	1.4646	$\bar{5}$	5	4
1	1.4443	1.4443	1	9	4
1	1.4390	1.4387	$\bar{2}$	2	12
1	1.4328	1.4325	0	0	12
<1	1.4308	1.4309	$\bar{3}$	5	10
<1	1.4165	1.4166	1	7	8
2	1.4083	1.4082	2	6	8
		1.4076	$\bar{2}$	6	10
3	1.4048	1.4051	$\bar{6}$	2	2
1	1.4012	1.4015	1	5	10
3	1.3959	1.3960	4	6	4
		1.3957	$\bar{1}$	9	6
		1.3953	$\bar{4}$	6	8
1	1.3786	1.3789	3	9	0
1	1.3755	1.3749	$\bar{4}$	8	2

Table 3. (continued).

I_{obs}	d_{obs}	d_{calc}	h	k	l	I_{obs}	d_{obs}	d_{calc}	h	k	l
6	1.9589	1.9582	2	6	2	2	1.3693	1.3691	2	8	6
		1.9577	$\bar{2}$	6	4	<1	1.3468	1.3466	3	7	6
5	1.9542	1.9555	$\bar{1}$	7	2	<1	1.3439	1.3438	$\bar{4}$	0	12
3	1.9494	1.9508	1	1	8	1	1.3294	1.3294	0	4	12
2	1.9283	1.9272	$\bar{4}$	0	6	1	1.3091	1.3086	$\bar{5}$	7	6
1	1.9066	1.9069	1	7	2	1	1.3057	1.3051	$\bar{3}$	9	6
<1	1.8935	1.8931	1	5	6			1.3040	$\bar{6}$	2	8
<1	1.8734	1.8735	3	5	2	1	1.2997	1.2994	6	4	0
1	1.8617	1.8618	4	2	2			1.2989	$\bar{6}$	4	6
1	1.8584	1.8606	$\bar{4}$	2	6	1	1.2893	1.2895	$\bar{1}$	9	8
3	1.8466	1.8461	$\bar{4}$	4	2	<1	1.2822	1.2824	1	11	0
2	1.8423	1.8408	0	4	8	1	1.2749	1.2753	$\bar{1}$	11	2
		1.8399	$\bar{1}$	7	4	<1	1.2635	1.2630	1	7	10
4	1.8309	1.8303	0	6	6	1	1.2485	1.2483	2	8	8
1	1.8056	1.8052	4	4	0	1	1.2452	1.2456	5	7	2
		1.8047	$\bar{4}$	4	4	1	1.2417	1.2410	$\bar{5}$	5	10
<1	1.8003	1.8011	$\bar{3}$	3	8	1	1.2400	1.2398	4	8	4
1	1.7898	1.7896	$\bar{3}$	5	6	1	1.2273	1.2272	0	6	12
2	1.7846	1.7844	0	8	0	1	1.2166	1.2165	1	11	4

of 24 h). Powder data were processed with the PANalytical High-Score software, used for the peak-profile fitting procedure (Pseudovoigt shape function corrected for asymmetry, after Thompson–Cox–Hastings). The unit-cell refinement was done with Celref software (Laugier & Bochu, 2004) using hkl-indices obtained from the structure model calculated by the program PowderCell (Kraus & Nolze, 1996). Refined parameters were lattice constants and the correction for the sample displacement. Unit-cell parameters refined from the powder pattern are $a = 8.6288(8)$ Å, $b = 14.2755(9)$ Å, $c = 18.720(1)$ Å, $\beta = 104.040(4)°$, $V = 2117.4(2)$ Å^3.

4.3. Single-crystal X-ray diffraction

The single-crystal study was conducted utilizing an Oxford Gemini diffractometer with Cu$K\alpha$ radiation ($\lambda = 1.540568$ Å) and a focused ~200-μm beam. The use of Cu$K\alpha$ source was necessary because of the crystal dimensions. The data collection provided the following unit cell: $a = 8.6201(17)$ Å, $b = 14.229(3)$ Å, $c = 8.8705(19)$ Å, $\beta = 103.998(18)°$, $V = 1055.7(4)$ Å^3 and $Z = 4$. The structure was solved from diffraction data and refined to an R of 8.77 % for 528 reflections with $I_{obs} > 3\sigma(I)$. However, the structure model was not complete and contained several peculiar features. First of all, the K atoms could not be located from the data, and difference Fourier maps contained a large number of positive peaks, principally around the U atoms. That was not unreasonable; considering that, the absorption linear coefficient was 92.51 mm^{-1} (for the Cu radiation). Therefore, a new diffraction experiment was undertaken in order to obtain better results. A prismatic, $40 \times 13 \times 10$ μm^3 crystal was selected for X-ray study employing a Rigaku Oxford diffraction SuperNova diffractometer. Mirror-mono-chromatized Mo$K\alpha$ radiation ($\lambda = 0.71073$ Å) from a microfocus X-ray source was used with an Atlas S2 CCD detector. Compared to the previous experiment, it was found out that we had missed some of the weak reflections responsible for the doubling of the c parameter. The new cell was related to the old cell by the matrix (1 0 0/0 1 0/0 0 2). The studied crystal is monoclinic, with $a = 8.6254(16)$, $b = 14.258(3)$, $c = 17.703(4)$ Å, $\beta = 104.052(18)$, $V = 2122.0(8)$ Å^3 and $Z = 8$ (Table 4). In comparison to the experiment on the Gemini diffractometer, the number of collected reflections on SuperNova instrument increased by a factor of about 14. Integration of the data, including corrections for background, polarization and Lorentz effects, were carried out with the CrysAlis RED program. The absorption correction, which combines the shape of the crystal and an empirical frame scaling, was done in Jana2006 (Petříček et al., 2014). The structure of plavnoite was solved by the charge-flipping algorithm using the Shelxt (Sheldrick, 2015). The structure was refined in the Jana2006 program (Petříček et al., 2014) by least squares based on F^2. The structure solution provided a reasonable model involving a nearly complete uranyl-sulfate sheet and several interstitial atom sites. The positions of the remaining atoms, oxygen and potassium were located on the difference-Fourier maps. The O site linked to one of the Mn sites possessed a significantly negative value for U_{iso}, suggesting the possibility that K partially occupied this site. The refined K/O occupancy at the site is about 50/50. The composition obtained from the structure model, with respect to the Me sites, $K_{0.532}Mn_{0.565}$, approaches the composition obtained by the EPMA study, $K_{0.75}Me^{2+}{}_{\Sigma 0.59}$ pfu. The oxygen atoms of the SO$_4$ groups had to be constrained to the same value of U_{iso}, because they otherwise were non-positive

Table 4. Summary of data collection condition, crystallographic details and structure refinement for plavnoite.

Structural formula	$K_{0.565}Mn_{0.532}[(UO_2)_2O_2(SO_4)](H_2O)_{2.44}$
Unit-cell parameters (from 617 reflections between 3.7 and 26.6 °θ)	$a = 8.6254(16)$ Å
	$b = 14.258(3)$ Å
	$c = 17.703(1)$ Å
	$\beta = 104.052(18)°$
V [Å^3]	2122.0(8)
Z	8
Space group	$C2/c$
$D_{calc.}$ [g cm^{-3}]	4.801 (for the above given formula)
Temperature	296 K
Wavelength	Mo$K\alpha$, 0.71073 Å
Crystal dimensions	$40 \times 13 \times 10\ \mu m^3$
Limiting θ angles	3.71–29.47°
Limiting Miller indices	$-11 \leq h < 11,\ -19 \leq k \leq 17,\ -23 \leq l \leq 24$
No. of reflections	11,747
No. of unique reflections	2653
No. of observed reflections (criterion)	989 [$I > 3\sigma(I)$]
Absorption coefficient (mm^{-1}), method	31.72, analytical + empirical scaling
T_{min}/T_{max}	0.980/1.000
R_{int} obs/all	0.0992/0.1679
F_{000}	2588
Param. refined, constraints, restraints	80, 3, 9
R_1, wR_2 (obs)	0.0499, 0.0998
R_1, wR_2 (all)	0.1745, 0.1618
GOF (obs, all)	0.90, 0.88
Weighting scheme	$1/(\sigma^2(I) + 0.0000004I^2)$
Twin matrix	$\begin{pmatrix} 1 & 0 & 0 \\ 0 & -1 & 0 \\ -0.997 & 0 & -1 \end{pmatrix}$
Twin fractions	0.544(3)/0.456(3)
$\Delta\rho_{min}$, $\Delta\rho_{max}$ (e Å^{-3})	−13.75, 8.73

definite. The crystal was found to be twinned, which is a common feature within this mineral group, with the monoclinic twin law (1 0 0/0 −1 0/−0.997 0 −1), providing a refined twin fraction of 0.544(3)/0.456(3). Implementation of the twinning in the refinement yielded a significant drop in the R values by about 4 %. The refinement converged to $R = 0.0499$ and $wR = 0.0998$ for 989 unique observed reflections. Final atom coordinates and displacement parameters are listed in Table 4, selected interatomic distances in Table 5, and the bond-valence analysis (after Brown, 1981, 2002) is given in Table 6. The original crystallographic information file is provided as Supplementary material linked to this article and freely available from the Geoscience Wolrd (GSW) website of the journal: http://eurjmin.geoscienceworld.org.

4.4. General crystal structure features

The crystal structure of plavnoite (Fig. 6) contains two independent U, two S, two Mn and fourteen O sites, including one mixed site occupied by K and O. The structure is consistent with the general features of zippeite-group minerals (Brugger *et al.*, 2003; Burns *et al.*, 2003; Plášil *et al.*, 2011a and b, 2013) and has the so-called zippeite topology (Burns, 2005). A detailed discussion on the topological features can be found in the aforementioned publications. The structural unit of the plavnoite structure − the uranyl oxo-sulfate sheets (unprotonated), of composition $[(UO_2)_2O_2(SO_4)]^{2-}$, are characteristic for the M^{2+}-containing monoclinic zippeites (Schindler & Hawthorne, 2008; Plášil *et al.*, 2013, 2014b). The interlayer of the plavnoite structure contains M^{2+} sites, occupied by Mn^{2+}, O sites of H_2O molecules and a mixed K/O site. The two symmetrically unique Mn sites are coordinated octahedrally in a distinct manner (Fig. 7). While the Mn1 site is linked to two H_2O sites (two symmetrically related O11 sites) and four O apical uranyl atoms in the structural units, the Mn2 site is linked to two uranyl O atoms and four H_2O sites (O11, O13, O14 and a mixed K/O site). The presence of K1 and Mn2 atoms is mutually exclusive. This leads to the logical question about the effective charge balance between the sheets and the interlayer (see below).

The structural formula obtained from the refinement is $K_{0.565}Mn_{0.532}[(UO_2)_2O_2(SO_4)](H_2O)_{2.44}$, $Z = 8$, with $D_{calc} = 4.801$ g cm^{-3}. We note that the H_2O content derived from the structure is lower than the ideal H_2O content (3.5H_2O) of M^{2+}-containing zippeite-like minerals with monoclinic symmetry (Burns *et al.*, 2003). It is probably actually lower than the ideal content, and it is most probably due to the K/O disorder; however, the refined K/O ratio can be affected to some extent by the

Table 5. Atom fractional coordinates and displacement parameters (U_{eq}, U_{iso}, U_{aniso}) for plavnoite.

Atom	x	y	z	$U_{eq/iso}$	U_{11}	U_{22}	U_{33}	U_{12}	U_{13}	U_{23}
U1	0.3331(4)	0.2318(3)	0.41472(18)	0.0084(10)	0.0051(17)	0.0106(12)	0.0085(15)	0.0017(19)	−0.0004(16)	0.0025(15)
U2	0.3300(4)	0.7687(3)	0.41546(17)	0.0077(9)	0.0081(18)	0.0127(13)	0.0037(14)	0.0007(18)	0.0038(16)	0.0018(15)
S1	0	0.2428(9)	0.25	0.0038(15)*						
S2	0.5	0.2367(10)	0.25	0.0038(15)*						
Mn1	0.5	0	0.5	0.011(4)*						
Mn2	0.327(2)	0.498(4)	0.3716(8)	0.011(4)*						
O1	0.113(4)	0.186(2)	0.305(2)	0.006(2)*						
O2	0.609(9)	0.255(2)	0.460(2)	0.006(2)*						
O3	0.093(8)	0.254(2)	0.450(2)	0.005(7)*						
O4	0.441(3)	0.1776(19)	0.3040(17)	0.006(2)*						
O5	0.336(5)	0.3567(18)	0.3931(19)	0.011(9)*						
O6/K1	0.5377(19)	0.501(4)	0.3478(7)	0.048(6)*						
O7	0.345(5)	0.107(3)	0.432(2)	0.001(9)*						
O8	−0.077(3)	0.3064(19)	0.2944(18)	0.006(2)*						
O9	0.331(7)	0.893(4)	0.434(3)	0.031(15)*						
O10	0.628(4)	0.301(2)	0.295(2)	0.006(2)*						
O11	0.377(2)	−0.002(5)	0.5848(10)	0.009(5)*						
O12	0.314(5)	0.6495(10)	0.3814(17)	0.003(8)*						
O13	0.212(4)	0.488(4)	0.248(2)	0.002(9)*						
O14	0.5	0.5	0.5	0.056(12)*						

* Refined occupancies: Mn1 = 0.49(2), Mn2 = 0.286(13), O6/K1 = 0.43(5)/0.57(5).

Table 6. Selected interatomic distances (in Å) in the plavnoite structure.

U1–O1	2.45(3)	U2–O2^{ii}	2.24(7)
U1–O2	2.34(7)	U2–O2^{iii}	2.17(4)
U1–O3	2.33(7)	U2–O3^{iv}	2.21(7)
U1–O3^i	2.33(3)	U2–O8^{iv}	2.52(3)
U1–O4	2.49(3)	U2–O10^{ii}	2.45(3)
U1–O5	1.82(3)	U2–O9	1.81(6)
U1–O7	1.80(4)	U2–O12	1.797(17)
$\langle$U1–O$_{Ur}\rangle$	1.81	$\langle$U2–O$_{Ur}\rangle$	1.80
$\langle$U1–O$_{eq}\rangle$	2.39	$\langle$U2–O$_{eq}\rangle$	2.32
S1–O1	1.45(3)	S2–O4	1.46(3)
S1–O1^v	1.45(3)	S2–O4^{vi}	1.46(3)
S1–O8	1.46(3)	S2–O10	1.50(3)
S1–O8^v	1.46(3)	S2–O10^{vi}	1.50(3)
$\langle$S1–O$\rangle$	1.46	$\langle$S2–O$\rangle$	1.48
Mn1–O7	2.19(4)	Mn2–O5	2.05(6)
Mn1–O7^x	2.19(4)	Mn2–O6	1.96(3)
Mn1–O9^{xi}	2.23(5)	Mn2–O11^i	2.08(3)
Mn1–O9^{iii}	2.23(5)	Mn2–O12	2.18(5)
Mn1–O11	2.04(2)	Mn2–O13	2.17(4)
Mn1–O11^x	2.04(2)	Mn2–O14	2.398(13)
$\langle$Mn1–O$\rangle$	2.15	$\langle$Mn2–O$\rangle$	2.14
K1–O1^{vii}	2.86(6)		
K1–O5	2.95(5)		
K1–O7	3.11(5)		
K1–O9	3.03(6)		
K1–O10	3.15(6)		
K1–O13	2.94(3)		
K1–O13^{viii}	3.05(4)		
K1–O14	2.792(13)		
K1–O12	3.02(5)		
$\langle$K1–O$\rangle$	2.99		

Fig. 6. The structure of plavnoite viewed along [1 0 0]. Uranyl sulfate sheets (UO$_7$ = blue, SO$_4$ = yellow) of the zippeite topology alternate with interlayer occupied by the Mn^{2+}-based distorted octahedra (orange) and a mixed K1/O6 site (violet). Unit-cell edges are outlined in red. (Online version in colour)

4.5. Plavnoite and zippeite group − structural and crystal chemical features

The coordination of the Mn^{2+} cations in the interlayer is very similar to that found in the structure of natural magnesiozippeite by Plášil *et al.* (2013). The presence of both K$^+$ and M^{2+} in the interlayer of the zippeite-group minerals and compounds is not surprising. First of all, the chemical data available for *zippeites* suggest a miscibility between M$^+$ and M^{2+} members, and the presence of both monovalent and divalent cations as interstitial species was documented for synthetic *zippeites* by single-crystal X-ray studies (Peeters *et al.*, 2008).

problems connected with site-scattering refinement of the light elements besides heavy elements (comparing the scattering power of O and K besides heavy scattering U).
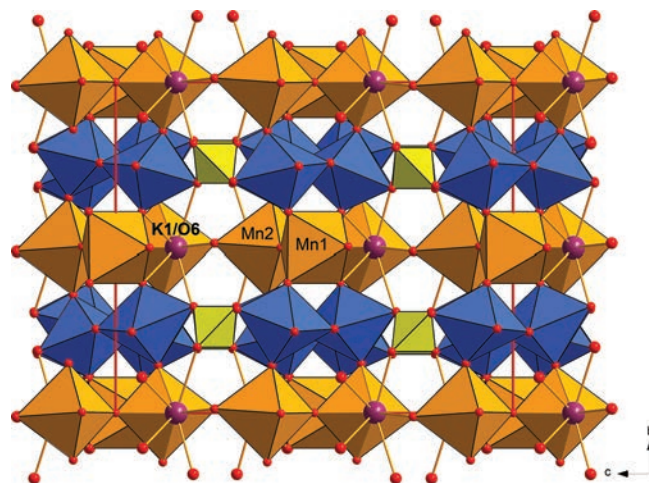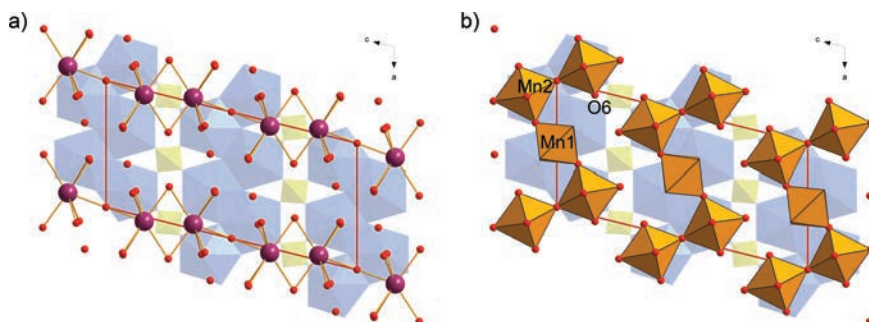
Fig. 7. The interstitial complex in the structure of plavnoite: (a) infinite chains of Mn^{2+}-octahedra extending along [1 0 0] alternate with (b) the K-based (violet atom) polyhedra extending along [0 0 1]. Both sites are partially occupied and mutually exclusive. Unit-cell edges are outlined in red. (Online version in colour)

Table 7. The bond-valence analysis for plavnoite.*

	U1	U2	Mn1	Mn2	K1	S1	S2	$\sum$BV	Assignment
O1	0.45				0.14	1.60×2↓		2.19	O
O2	0.56	0.68, 0.78						2.04	O
O3	1.14	0.72						1.86	O
O4	0.42						1.56×2↓	1.98	O
O5	1.55			0.50	0.11			2.16	O
O6				0.63				0.63	H_2O
O7	1.62		0.34×2↓		0.11			2.07	O
O8		0.39				1.56×2↓		1.95	O
O9		1.59	0.31×2↓		0.17			2.07	O
O10		0.45			0.06		1.40×2↓	1.91	O
O11			0.51×2↓	0.46				0.97	H_2O
O12		1.63		0.35	0.09			2.07	O
O13				0.36	0.08			0.44	H_2O
O14				0.19	0.17			0.36	H_2O
$\sum$BV	5.75	6.25	2.31	2.48	0.94	6.32	5.91		

* Values are given in valence units (vu). $\sum$BV = sum of bond-valences incident at the atomic site; ×2↓ = multiplicity. U^{6+}–O bond-valence parameters ($r_0 = 2.045$, $b = 0.51$) taken from Burns *et al.* (1997) for $^{[7]}$U–O; Mn^{2+}–O, S^{6+}–O and K–O bond-valence parameters from Brown & Altermatt (1985).

Although plavnoite is structurally very similar to those synthetic compounds (Table 7), it differs from them in some details. At first sight, there is a clear difference in the chemical composition of these structures: according to the structure refinement, plavnoite contains $K_{0.57}Mn_{0.53}$ ($K_{0.75}Me^{2+}_{\Sigma0.59}$ according to EPMA), while the synthetic K–Mn zippeite contains $K_{0.50}Mn_{0.75}$ ($K_{0.19}Mn_{0.67}$ according to EPMA, Peeters *et al.*, 2008). Comparing the structure of plavnoite with the structures of the zippeite-related compounds synthesized by Peeters *et al.* (2008), it shows significant differences in the interlayer complex. The interstitial cations are ordered in a distinct way, which is reflected in the composition of the interstitial complex, as well (see above). Although in the case of the synthetic compound Mn^{2+} (and other divalent metals in the series of synthetic compounds) is dominant, in plavnoite K^+ is dominant over M^{2+}. The charge imbalance due to the vacancies at the sites occupied by monovalent and divalent cations (taking into account their lowered occupancy) is, most

probably, responsible for the protonation of some of the O^{2-} anions within the structural unit. However, according to the bond-valence analysis, and as it is clear from the average structure, none of the O atoms within the structural sheet has an OH character, they are just acceptors of the H-bonds from an interlayer.

Plavnoite is a new member of the uranyl sulfates of the zippeite group, Strunz class 07.EC, Dana class 31.10.04. Although it contains potassium, it differs substantially from zippeite, ideally $K_x[(UO_2)_4(SO_4)_2O_x(OH)_{4-x}]$ $(H_2O)_{6-x}$ (where $x \approx 2$ in case of natural mineral) (Plášil *et al.*, 2011a). The differences are in the configuration and composition of the interstitial complex and in the composition of the structural sheets. Plavnoite is very similar to the synthetic zippeite-group-related phases described by Peeters *et al.* (2008), which are monoclinic (space group *C*2/*c*) and contains K and a divalent transition metal (Co, Ni, Zn or Mn) in their structures. These structures differ from those of zippeite (Burns *et al.*, 2003; Plášil *et al.*, 2011a) and synthetic magnesiozippeite (Burns

Table 8. Comparative data for the relevant members of the zippeite group of minerals.

	Plavnoite	Zippeite	Magnesiozippeite	Magnesiozippeite (synth.)	Mn–K zippeite (synth.)
Type locality	Jáchymov, CZ	Jáchymov, CZ			
Reference	This paper	Plášil et al. (2011a)	Plášil et al. (2013)	Burns et al. (2003)	Peeters et al. (2008)
M metal (ideal.)	$K_{0.8}Mn_{0.6}$	K	Mg	Mg	$Mn_{0.75}K_{0.5}$*
M metal (meas.)	$K_{0.75}(Mn_{0.50}Zn_{0.04}Ni_{0.03}Mg_{0.02})_{\Sigma 0.59}$	$(K_{1.73}Fe_{0.0}Ca_{0.02}\ldots)_{\Sigma 1.82}$	$(Mg_{0.51}Co_{0.07}Zn_{0.05}Ca_{0.04}K_{0.04}\cdots)_{\Sigma 0.74}$	–	$(Mn_{0.68}K_{0.19})_{\Sigma 0.87}$
OH^{su}	No	Yes	No	No	No
Space group	C2/m	C2/m	C2/m	C2/m	C2/c
a	8.6254(16)	8.7802(6)	8.7005(5)	8.6514(4)	8.661(6)
b	14.258(3)	13.9903(12)	14.2541(6)	14.1938(7)	14.375(8)
c	17.703(1)	8.8630(6)	8.8433(5)	17.7211(9)	17.705(12)
β	104.052(18)	104.524(7)	104.408(5)	104.131(1)	104.12(5)
V	2122.0(8)	1053.92(12)	1062.24(9)	2110.24(18)	2138(2)
Z	8	2	4	8	8
Strongest lines in XRD powder pattern	8.595/27 7.133/100 3.565/25 3.446/36 3.104/47	8.578/21# 6.998/100 3.500/26 3.476/19 3.113/42	8.568/22# 7.133/100 3.566/20 3.467/22 3.113/27	7.222/4# 7.097/80 3.548/100 3.104/60 2.878/29	8.858/2# 5.551/43 3.594/100 3.112/81 2.862/26

*From the structure; #calculated from structure data. OH^{su} is the presence of OH within the structural unit.

et al., 2003), and they contain a M^{2+}-polyhedron linked in a manner similar to that in the structure of natural magnesiozippeite (Plášil et al., 2013). The K:M^{2+} ratio seems to be variable and also correlates with the number of O atoms in the structural sheets, probably with a small amount of OH$^-$ for charge balance. The comparative data for the relevant members of the zippeite group are given in Table 8. Plavnoite is structurally more similar to monoclinic zippeites that contain divalent metal cations than it is to triclinic members of the group, sejkoraite-(Y) (Plášil et al., 2011b) or marécottite (Brugger et al., 2003) or to zippeite (Plášil et al., 2011a) itself. Based on the current knowledge, we can summarize that there is most probably no complete solid solution between K- and Mn-dominant zippeite; plavnoite (with a slightly variable composition) actually represents an ordered stable member. According to our best knowledge, there is no K-dominant zippeite, natural or synthetic, that contains structural units similar to the monoclinic M^{2+}-containing members, and there is no Mn^{2+}-dominant member of the zippeite group, as well.

References

Bartlett, J.R. & Cooney, R.P. (1989): On the determination of uranium-oxygen bond lengths in dioxouranium(VI) compounds by Raman spectroscopy. *J. Mol. Struct.*, **193**, 295–300.

Brown, I.D. (1981): The bond-valence method: an empirical approach to chemical structure and bonding. *in* "Structure and bonding in crystals", M. O'Keeffe and A. Navrotsky, eds. Academic Press, New York, Vol. 2, 1–30.

Brown, I.D. (2002): The chemical bond in inorganic chemistry. The bond valence model. Oxford University Press, Oxford.

Brown, I.D. & Altermatt, D. (1985): Bond-valence parameters obtained from a systematic analysis of the inorganic crystal structure database. *Acta Crystallogr.*, **B41**, 244–248.

Brugger, J., Meisser, N., Burns, P.C. (2003): Contribution to the mineralogy of acid drainage of uranium minerals: marecottite and the zippeite-group. *Am. Mineral.*, **88**, 676–685.

Brugger, J., Wallwork, K.S., Meisser, N., Pring, A., Ondruš, P., Čejka, J. (2006): Pseudojohannite from Jáchymov, Musunoï and La Creusaz: a new member of the zippeite group. *Am. Mineral.*, **91**, 929–936.

Burns, P.C. (2005): U^{6+} minerals and inorganic compounds: insights into an expanded structural hierarchy of crystal structures. *Can. Mineral.*, **43**, 1839–1894.

Burns, P.C., Ewing, R.C., Hawthorne, F.C. (1997): The crystal chemistry of hexavalent uranium: polyhedron geometries, bond-valence parameters, and polymerization of polyhedra. *Can. Mineral.*, **35**, 1551–1570.

Burns, P.C., Deely, K.M., Hayden, L.A. (2003): The crystal chemistry of the zippeite group. *Can. Mineral.*, **41**, 687–706.

Čejka, J. (1999): Infrared spectroscopy and thermal analysis of the uranyl minerals. *in* "Uranium: mineralogy, geochemistry and the environment", P.C. Burns and R.C. Ewing, eds. *Rev. Mineral. Geochem.*, **38**, 521–622.

Frondel, C., Ito, J., Honea, R.M., Weeks, A.M. (1976): Mineralogy of the zippeite group. *Can. Mineral.*, **14**, 429–436.

Hloušek, J., Plášil, J., Sejkora, J., Škácha P. (2014): News and new minerals from Jáchymov, Czech Republic (2003–2014). *Bull. mineral.-petrolog. odd. Nár. Muz. (Praha)*, **22**, 155–181.

Krivovichev, S.V. & Plášil, J. (2013): Mineralogy and crystallography of uranium. *in* "Uranium, from cradle to grave", P.C. Burns and G.E. Sigmon, eds. *MAC Short Course*, **43**, pp. 15–119, Winnipeg MB, May 2013.

Kraus, W. & Nolze, G. (1996): POWDER CELL − a program for the representation and manipulation of crystal structures and calculation of the resulting X-ray powder patterns. *J. Appl. Cryst.*, **29**, 301–303.

Laugier, J. & Bochu, B. (2004): LMPG suite of programs for the interpretation of X-ray experiments. ENSP/Laboratoire des Matériaux et du Génie Physique, BP 46, 38042 Saint Martin d'Hères, France. http://www.ccp14.ac.uk/tutorial/lmgp/ (accessed: 16.01.2014).

Libowitzky, E. (1999): Correlation of O–H stretching frequencies and O–H$\cdots$O hydrogen bond lengths in minerals. *Monatsh. Chem.*, **130**, 1047–1059.

Ondruš, P., Veselovský, F., Hloušek, J., Skála, R., Vavřín, I., Frýda, J., Čejka, J., Gabašová, A. (1997): Secondary minerals of the Jáchymov (Joachimsthal) ore district. *J. Czech Geol. Soc.*, **42**, 3–76.

Ondruš, P., Veselovský, F., Gabašová, A., Hloušek, J., Šrein, V., Vavřín, I., Skála, R., Sejkora, J., Drábek, M. (2003): Primary minerals of the Jáchymov ore district. *J. Czech Geol. Soc.*, **48**, 19–147.

Peeters, M.O., Vochten, R., Blaton, N. (2008): The crystal structures of synthetic potassium-transition metal zippeite-group phases. *Can. Mineral.*, **46**, 173–182.

Petříček, V., Dušek, M., Palatinus, L. (2014): Crystallographic computing system Jana2006: general features. *Z. Kristallogr.*, **229**, 345–352.

Plášil, J. (2014): Oxidation-hydration weathering of uraninite: the current state-of-knowledge. *J. Geosci.*, **59**, 99–114.

Plášil, J., Buixaderas, E., Čejka, J., Sejkora, J., Jehlička, J., Novák, M. (2010): Raman spectroscopic study of the uranyl sulphate mineral zippeite: low wavenumber and U–O stretching regions. *Anal. Bioanal. Chem.*, **397**, 2703–2715.

Plášil, J., Mills, S.J., Fejfarová, K., Dušek, M., Novák, M., Škoda, R., Čejka, J., Sejkora, J. (2011a): The crystal structure of natural zippeite, $K_{1.85}H^{+}_{0.15}[(UO_2)_4O_2(SO_4)_2(OH)_2](H_2O)_4$, from Jáchymov, Czech Republic. *Can. Mineral.*, **49**, 1089–1103.

Plášil, J., Dušek, M., Novák, M., Čejka, J., Císařová, I., Škoda, R. (2011b): Sejkoraite-(Y), a new member of the zippeite group containing trivalent cations from Jáchymov (St. Joachimsthal), Czech Republic: description and crystal structure refinement. *Am. Mineral.*, **96**, 983–991.

Plášil, J., Fejfarová, K., Wallwork, K.S., Dušek, M., Škoda, R., Sejkora, J., Čejka, J., Veselovský, F., Hloušek, J., Meisser, N., Brugger, J. (2012): Crystal structure of pseudojohannite, with a revised formula, $Cu_3(OH)_2[(UO_2)_4O_4(SO_4)_2](H_2O)_{12}$. *Am. Mineral.*, **97**, 1796–1803.

Plášil, J., Fejfarová, K., Škoda, R., Dušek, M., Čejka, J., Marty, J. (2013): The crystal structure of magnesiozippeite, $Mg[(UO_2)_2O_2(SO_4)](H_2O)_{3.5}$, from East Saddle Mine, San Juan County, Utah (U.S.A.). *Mineral. Petrol.*, **107**, 211–219.

Plášil, J., Veselovský, F., Hloušek, J., Škoda, R., Novák, M., Sejkora, J., Čejka, J., Škácha, P., Kasatkin, A.V. (2014a): Mathesiusite, $K_5(UO_2)_4(SO_4)_4(VO_5)(H_2O)_4$, a new uranyl vanadate-sulfate from Jáchymov, Czech Republic. *Am. Mineral.*, **99**, 625–632.

Plášil, J., Dušek, M., Čejka, J., Sejkora, J. (2014b): The crystal structure of rabejacite, the Ca^{2+}-dominant member of the zippeite group. *Mineral. Mag.*, **57**, 1249–1263.

Plášil, J. & Škoda, R. (2015): New crystal-chemical data for marécottite. *Mineral. Mag.*, **79**, 649–660.

Pouchou, J.L. & Pichoir, F. (1985): "PAP" (φρZ) procedure for improved quantitative microanalysis. *in* "Microbeam analysis", J.T. Armstrong, ed. San Francisco Press, San Francisco, CA, 104–106.

Schindler, M. & Hawthorne, F.C. (2008): The stereochemistry and chemical composition of interstitial complexes in uranyl-oxysalt minerals. *Can. Mineral.*, **46**, 467–501.

Sheldrick, G.M. (2015): SHELXT − integrated space-group and crystal-structure determination. *Acta Crystallogr.*, **A71**, 3–8.